

Study of salt effects in ultrasonication-assisted spray ionization mass spectrometry

Dear Sir,

Ultrasonication-assisted spray ionization mass spectrometry (UASI-MS)^[1,2] is a recently developed technique. The UASI-MS requires only an inexpensive ultrasonicator and a tapered capillary for the generation of gas-phase ions from liquid samples at atmospheric pressure. No external voltage is connected to the UASI capillary emitter, which is close (~5 mm) to the orifice of a mass spectrometer. Ultrasonication drives the liquid sample from the inlet to the capillary outlet followed by formation of fine droplets, and gas-phase ions are then generated for MS analysis. UASI-MS is suitable for the analysis of a wide mass range of biomolecules, such as amino acids, peptides, and proteins.^[1] A notable advantage of coupling UASI for MS analysis is relatively low ion background observed in the UASI mass spectra. In conventional electrospray ionization (ESI) MS, background ions resulting from electrochemical reduction/oxidation of solvent are unavoidable because of the use of high voltages on the sample emitter to generate electrospray. Alternatively, ultrasonication is used to assist the generation of very fine droplets from the outlet of a tapered capillary in the UASI-MS without applying any electric connection in the UASI capillary emitter. The capillary outlet is close to the orifice of the mass spectrometer, which is applied with a high voltage. Thus, we believe that the generated fine droplets are polarized on the way to the orifice of the mass spectrometer.^[3] A floating potential was therefore generated. After subsequent solvent evaporation, the polarized droplets shrink followed by disruption because of coulombic repulsion resulting from the increase of the charge density, leading the formation of smaller droplets with net positive charges, neutral state, and net negative charges. The positively charged droplets tend flying to the orifice of the mass spectrometer applied with a negative potential. After desolvation, gas-phase ions are readily formed for MS analysis. Owing to the ease of polarization, the formation of very fine droplets is a prerequisite for successful generation of multiply/singly charged ions when no electrode/voltage is applied on the sample emitter as demonstrated in several reports.^[1,2,4-7] In the UASI-MS, ultrasonication is significant for the assistance of the formation of fine droplets. The elimination of the use of high voltages in the UASI approach also leads the reduction of background ions. In this work, UASI-MS is further employed for the analysis of saccharides and samples containing high concentrations of salts. The salt effects of UASI-MS are investigated in this study.

An ultrasonicator (2.5 l, 160 W, 42 kHz), generally filled with 2.1 l of water, was used in the UASI setup. A capillary was tapered to have a sharp tip. The tapered capillary (length, 20 cm; tip diameter, ca. $10 \pm 3 \mu\text{m}$) was filled with the sample solution before being placed in an aqueous sample solution within a vial in the ultrasonicator (Fig. 1). The tapered capillary outlet was close (~5 mm) to the inlet of an Esquire 2000 ion trap mass

spectrometer (Bruker Daltonics, Bremen, Germany). No electric connection was made in the UASI capillary. The temperature of the heated transfer glass capillary in the mass spectrometer was maintained at 150 °C. The voltages on the MS capillary inlet were set at -1500 V for the spectra recorded in positive ion mode. The UASI signals were readily acquired when the ultrasonicator was switched on. A microTOF II focus MS (Bruker Daltonics, Germany; mass accuracy, <2 ppm; mass resolution, >16 500 FWHM) was used to confirm the mass of the ions generated from the UASI process. When the commercial spray emitter (i.d. = ~50 μm) was used for conducting ESI-MS analysis in positive ion mode, the spray voltage applied on the MS capillary inlet was set at -4 kV and the ESI emitter was grounded. The flow rate for sample infusion was set at 5 μl/min, the pressure of the nebulizer gas was set at 10 psi, and the temperature of the heated transfer capillary was maintained at 300 °C with a dry gas flow (5 l/min).

Figures 2(a) and 2(b) display the ESI and UASI mass spectra of glucose, respectively. Sodium ion adducts of glucose at m/z 203 dominate the ESI mass spectrum, whereas the UASI mass spectrum is dominated by the peak at m/z 198. A high-resolution microTOF was used to obtain the accurate mass of the peak at m/z 198 and confirm its identity. The mass was identified as 198.0980, which possibly corresponds to the ammonium ion adducts of glucose (exact mass of $\text{C}_6\text{H}_{16}\text{NO}_6 = 198.0972$). Furthermore, the UASI mass spectrum contains fewer background ions compared with that of the ESI. Unlike in the ESI-MS analysis, glucose favors binding with ammonium ions in the UASI-MS analysis, although no additional ammonium ions were added to the glucose sample. We believe that ammonia may come from ambient air, mainly contributed by human breath, which is usually at ppb concentration level.^[8] Although only a trace amount of ambient ammonia is available, it is sufficient for the formation of ammonium ion adducts of glucose in the UASI-MS analysis. Presumably, ammonium ions were formed in the UASI fine droplets after ambient ammonia fused with the droplets during the UASI processes. To further confirm the source of ammonia, we tried to lower the concentration of ammonia at ambient level during the UASI-MS analysis by purging nitrogen gas in the area between the UASI capillary outlet and the orifice of the mass spectrometer. As we expected, the intensity of the ammonium ion adducts of glucose declined significantly in the UASI mass spectra (results not shown). The result provides evidence that ammonia mainly comes from ambient air. Furthermore, when either methanol or ethanol was used as the solvent, the ammonium ion adducts of glucose still dominated the mass spectra (results not shown). The results imply that it is unlikely that the source of

* Correspondence to: Yu-Chie Chen, Department of Applied Chemistry, National Chiao Tung University, Hsinchu 300, Taiwan. E-mail: yuchie@mail.nctu.edu.tw

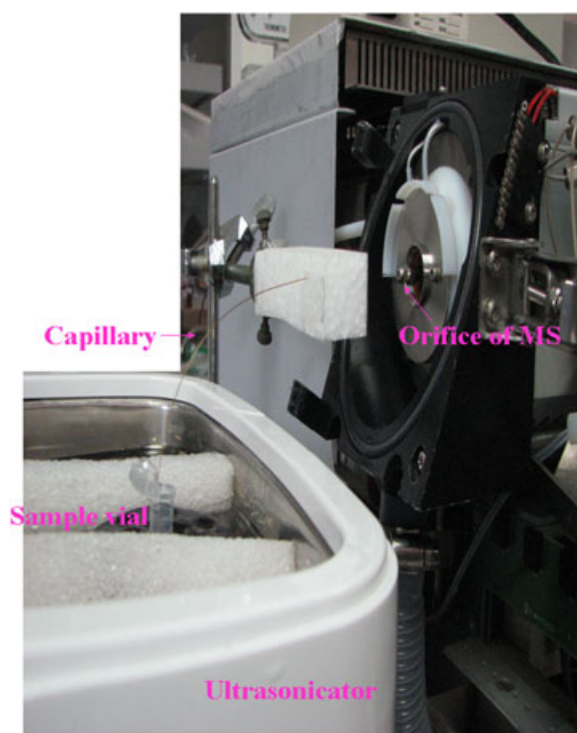


Figure 1. Photograph of the UASI-MS setup.

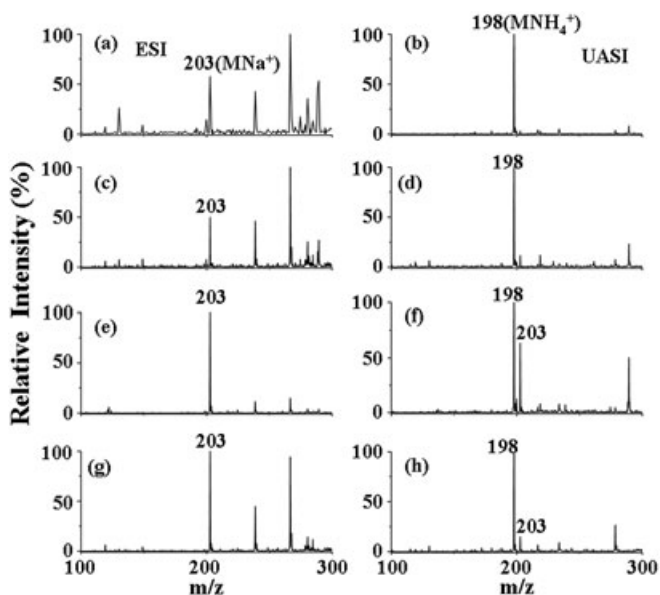


Figure 2. ESI and UASI mass spectra of glucose (0.1 mM) prepared in water/acetonitrile (1:1, v/v) containing (a, b) no salts, (c, d) 1 mM ammonium acetate, (e, f) 1 mM sodium acetate/1 mM ammonium acetate, and (g, h) 1 mM sodium acetate/10 mM ammonium acetate.

ammonium ions is from organic solvents. Glucose samples were prepared in solvent containing different concentrations of sodium acetate and ammonium acetate for the investigation of the salt-binding tendency of glucose. The samples were individually prepared in aqueous solutions containing 1 mM ammonium acetate, 1 mM sodium acetate/1 mM ammonium acetate, and 1 mM sodium acetate/10 mM ammonium acetate and then examined using ESI-MS and UASI-MS. The sodiated glucose peak at m/z 203 dominates

all the ESI mass spectra [Figs. 2(c), 2(e), and 2(g)]. However, the ammonium ion adduct of glucose at m/z 198 remains the base peak in all the UASI mass spectra [Figs. 2(d), 2(f), and 2(h)]. In the presence of sodium acetate [Figs. 2(f) and 2(h)], the ammonium ion adduct of glucose at m/z 198 remains the base peak and is adjacent to a weak sodiated glucose peak in the UASI mass spectra, indicating that glucose prefers to bind with ammonium ions in the UASI-MS analysis. UASI-MS has a high tolerance for sodium ions, as shown by the relatively low intensity of the sodiated glucose peak compared with the results obtained from conventional ESI-MS. This observation may result from much smaller droplets generated from the UASI compared with those obtained from conventional ESI because of the use of a very thin capillary tip (tip diameter: ca. $10 \pm 3 \mu\text{m}$) as the spray emitter in the UASI-MS. Small droplets can only contain limited amounts of sodium ions, leading to a relatively weak sodiated peak in the UASI mass spectra. For the samples containing high concentrations of salts, salt precipitation was observed in the outlet of the UASI capillary tip after the UASI-MS analysis. In addition, the ionization process in the UASI-MS appears soft, as shown by the intact ammonium ion remaining attached to the neutral saccharide structures. Generally, only protons can remain on the saccharide molecules during conventional ESI-MS analysis in the presence of additional ammonium salts.^[9,10] In addition, Wu *et al.* used an ultrasonic transducer with the frequency of 1.7 MHz to assist generation of an N-linked high-mannose-type oligosaccharide mannose 8 derivative (Man8, chemical formula: $\text{C}_{53}\text{H}_{93}\text{NO}_4$) in ultrasound-assisted spray MS.^[11] No molecular ions were observed in the mass spectrum, unless additional acid was spiked in the sample. Unlike our results, protonated pseudomolecular ions of Man8 appeared in the mass spectrum. It is understandable that sodiated adducts were not observed in the mass spectrum because Man8 is not a neutral saccharide. Nitrogen containing saccharides generally favors binding with protons owing to the high proton affinity. *In situ* desalting effects have also been observed in several ionization techniques such as desorption electrospray ionization (DESI)^[12,13] and fused-droplet electrospray ionization (FD-ESI).^[14] The desalting effects rely either on the polarities of ESI solvents or the formation of fine droplets.

Alkali metal (e.g. sodium or potassium) ion adducts of neutral saccharides generally dominate the mass spectra during ESI and MALDI MS analysis,^[15–19] whereas protonated neutral saccharides are rarely obtained. Alkali metal ion adducts of neutral saccharides are hardly fragmented in MS/MS analysis.^[10] The addition of ammonium salts to saccharide samples is helpful for the MS/MS analysis of saccharides.^[9] However, the addition of ammonium salts can be eliminated because the ammonium ion adducts of saccharides dominate the UASI mass spectra even when no additional ammonium salts are added in the samples. Figure 3(a) displays the ESI MS/MS spectrum of glucose when the peak at m/z 203 was used as the precursor ion. No fragment ions were observed in the mass spectrum. However, fragmentations in the UASI MS/MS spectrum of glucose were observed when the ammonium adduct of glucose at m/z 198 was used as the precursor ion. The peak at m/z 180 corresponds to the intact glucose. The peaks at m/z 163, 145, and 127 are due to the systematic loss of individual water molecules from the structure of glucose [Fig. 3(b)]. Directly employing UASI for the MS/MS analysis of glucose is suitable because of the unique preferential formation of the ammonium ion adducts of glucose even when no additional ammonium ion adducts are present in the sample.

Crown ethers were also used as model samples. Crown ethers exhibit high electronegativity of oxygen atoms, which can act as

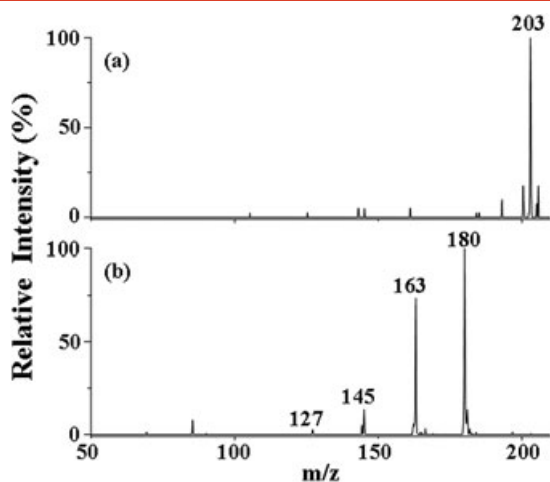


Figure 3. (a) ESI MS/MS spectrum at m/z 203 and (b) UASI MS/MS spectrum at m/z 198.

binding sites for metal ions^[20] and ammonium ions^[21] through ion-dipole interactions. Figure 4(a) displays the ESI mass spectrum of 15-crown-5, whereas Fig. 4(b) presents its UASI mass spectrum. The potassium ion adduct of 15-crown-5 at m/z 259 dominates the ESI mass spectrum [Fig. 4(a)]. The peak at m/z 238 corresponding to the ammonium ion adducts of 15-crown-5 also appears in the same ESI mass spectrum. The peak at m/z 238 dominates the UASI mass spectrum of 15-crown-5 [Fig. 4(b)]. Similarly, when 18-crown-6 was used as the sample, its potassium ion adduct peak at m/z 303 dominates the ESI mass spectrum [Fig. 4(c)], and its ammonium adduct peak at m/z 282 remains the base peak in the UASI mass spectrum [Fig. 4(d)]. No potassium ion adducts of crown ethers were observed in the UASI mass spectra. The ammonium ion adduct of 18-crown-6 still dominates the UASI mass spectrum even when the formation constant of 18-crown-6 with potassium ions is higher than that with ammonium ions.^[20,21] This result may be due to the low amount of available alkali metal ions in the small UASI droplets. However, the crown ether-derived ammonium ion adducts can be readily formed in the gas phase because of the presence of ammonia at ambient conditions, presumably from human breath.

The salt tolerance of UASI-MS was also investigated using bradykinin as the model sample. The doubly charged bradykinin ion peak at m/z 531 ($[M + 2H]^{2+}$) dominates both the ESI [Fig. 5(a)] and UASI [Fig. 5(b)] mass spectra when no additional salts were

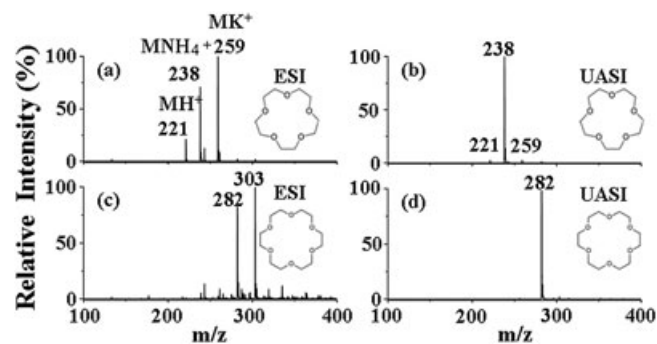


Figure 4. (a) ESI and (b) UASI mass spectra of 15-crown-5 (10^{-5} M, MW = 220) prepared in water/acetonitrile (1:1, v/v). (c) ESI and (d) UASI mass spectra of 18-crown-6 (10^{-5} M, MW = 264) prepared in water/acetonitrile (1:1, v/v).

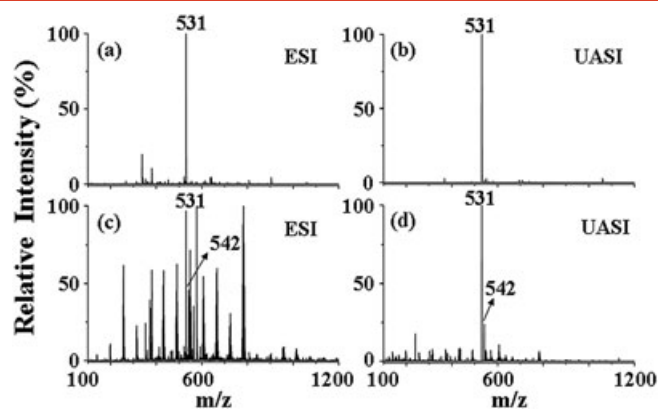


Figure 5. (a) ESI and (b) UASI mass spectra of bradykinin (10^{-6} M) prepared in water/acetonitrile (1:1, v/v). (c) ESI and (d) UASI mass spectra of bradykinin (10^{-6} M) prepared in water/acetonitrile (1:1, v/v) containing 10 mM sodium chloride.

added to the bradykinin sample. Fewer background ions are found in Fig. 5(b) compared with Fig. 5(a). The quality of the ESI mass spectrum is significantly affected when sodium chloride (10 mM) was spiked into the bradykinin sample. The doubly charged bradykinin ion peak at m/z 531 ($[M + 2H]^{2+}$) is surrounded by many sodium-chloride-derived ion peaks, and the sodiated bradykinin ion peak at m/z 542 ($[M + Na + H]^{2+}$) with a low intensity appears in the same mass spectrum [Fig. 5(c)]. However, the doubly charged bradykinin ion peak at m/z 531 still dominates the UASI mass spectrum [Fig. 5(d)] using the same sample for obtaining Fig. 5(c). The intensity of the background ions mainly derived from sodium chloride is relatively low in Fig. 5(d) compared with that observed in Fig. 5(c), demonstrating that the salt tolerance of the UASI-MS is superior to that of ESI-MS.

To determine the performance of the UASI analysis under a high-salt condition, such as in biological fluid samples, bradykinin was spiked into a 50-fold diluted urine sample. Figure 6(a) shows the ESI mass spectrum of the bradykinin sample, whereas Fig. 6(b) displays the corresponding UASI mass spectrum. The spectral quality of the ESI mass spectrum is considerably lower than that of the UASI mass spectrum in terms of the signal to noise ratios. The intensity of the doubly charged bradykinin peaks at m/z 531

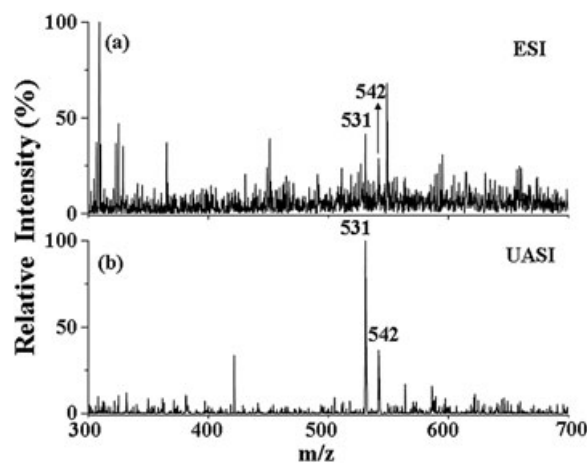


Figure 6. (a) ESI and (b) UASI mass spectra of bradykinin (10^{-5} M) spiked in diluted urine. The urine sample was mixed with equal volume of acetonitrile before conducting UASI-MS analysis.

$[(M + 2H)^{2+}]$ and $542 [(M + Na + H)^{2+}]$ in the ESI mass spectrum is relatively low compared with those observed in the UASI mass spectrum. Hence, UASI-MS analysis is more suitable for use in high-salt samples than is the conventional ESI-MS analysis, and additional desalting steps may not be necessary in the UASI-MS analysis because of its high-salt tolerance.

In conclusion, the current study demonstrated two unique features of the UASI-MS, namely, the preferential formation of ammonium ion adducts and the high-salt tolerance. Ammonium ion adducts in the UASI mass spectra are favorably formed if the samples contain oxygen-rich functional groups such as hydroxyls and ethers, whereas alkali ion adducts usually dominate the ESI mass spectra when the same samples are analyzed. In addition to these unique properties, the advantages of the UASI-MS, including simple sample preparation, low background ions, and high-salt tolerance, make this approach highly appropriate for the MS/MS analysis of neutral saccharides and high-salt samples.

Acknowledgements

We thank the National Science Council of Taiwan for the financial support of this work. We also thank Prof. Jan Sunner for helpful discussion.

Yours,

TA-JU LO, TSUNG-YI CHEN, YU-CHIE CHEN*

Department of Applied Chemistry, National Chiao Tung University, Hsinchu 300, Taiwan

References

- [1] Chen T. Y., Lin J. Y., Chen Y. C. Ultrasonication-assisted spray ionization mass spectrometry for the analysis of biomolecules in solution. *J. Am. Soc. Mass Spectrom.* **2010**, *21*, 1547.
- [2] Chen T. Y., Chao C. S., Mong K. K. T., Chen Y. C. Ultrasonication-assisted spray ionization mass spectrometry for on-line monitoring of organic reactions. *Chem. Commun.* **2010**, *46*, 8347.
- [3] Personal communication with Prof. Pawel Urban.
- [4] Takats Z., Wiseman J. M., Gologan B., Cooks R. G. Mass spectrometry sampling under ambient conditions with desorption electrospray ionization. *Science* **2004**, *206*, 471–473.
- [5] Hsieh C. H., Chang C. H., Urban P. L., Chen Y. C. Capillary action-supported contactless atmospheric pressure ionization for the combined sampling and mass spectrometric analysis of biomolecules. *Anal. Chem.* **2011**, *83*, 2866–2869.
- [6] Santos V. G., Regiani T., Dias F. F. G., Romão W., Jara J. L. P., Klitzke C. F., Coelho F., Eberlin M. N. Venturi easy ambient sonic-spray ionization. *Anal. Chem.* **2011**, *83*, 1375–1380.
- [7] McEwen C. N., Pagnotti V. S., Inutan E. D., Trimpin S. New paradigm in ionization: multiply charged ion formation from a solid matrix without a laser or voltage. *Anal. Chem.* **2010**, *82*, 9164–9168.
- [8] Špan I. P., Dryahina K., Smith D. Acetone, ammonia and hydrogen cyanide in exhaled breath of several volunteers aged 4–83 years. *J. Breath Res.* **2007**, *1*, 011001.
- [9] Madhusudan K. P. Tandem mass spectra of ammonium adducts of monosaccharides: differentiation of diastereomers. *J. Mass Spectrom.* **2006**, *41*, 1096.
- [10] March R. E., Stacey C. J. A tandem mass spectrometric study of saccharides at high mass resolution. *Rapid Commun. Mass Spectrom.* **2005**, *19*, 805.
- [11] Wu C. I., Wang Y. S., Chen N. G., Wu C. Y., Chen C. H. Ultrasound ionization of biomolecules. *Rapid Commun. Mass Spectrom.* **2010**, *24*, 2569–2574.
- [12] Zhang Y., Chen H. Detection of saccharides by reactive desorption electrospray ionization (DESI) using modified phenylboronic acids. *Int. J. Mass Spectrom.* **2010**, *289*, 98–107.
- [13] Chan C. C., Bolgar M. S., Miller S. A., Attygalle A. B. Evading metal adduct formation during desorption-ionization mass spectrometry. *Rapid Commun. Mass Spectrom.* **2010**, *24*, 2838–2842.
- [14] Chang D. Y., Lee C. C., Shiea J. Detecting large biomolecules from high-salt solutions by fused-droplet electrospray ionization mass spectrometry. *Anal. Chem.* **2002**, *74*, 2465–2469.
- [15] Zidkova J., Chmelik J. Determination of saccharides in fruit juices by capillary electrophoresis and matrix-assisted laser desorption/ionization time-of-flight mass spectrometry. *J. Mass Spectrom.* **2001**, *36*, 417.
- [16] Cmelik R., Stikarovska M., Chmelik J. Different behavior of dextrans in positive-ion and negative-ion mass spectrometry. *J. Mass Spectrom.* **2004**, *39*, 1467.
- [17] Chen C. T., Chen Y. C. Molecularly imprinted TiO₂-matrix-assisted laser desorption/ionization mass spectrometry for selectively detecting α -cyclodextrin. *Anal. Chem.* **2004**, *76*, 1453.
- [18] Wu H. P., Yu C. J., Lin C. Y., Lin Y. H., Tseng W. L. Gold nanoparticles as assisted matrices for the detection of biomolecules in a high-salt solution through laser desorption/ionization mass spectrometry. *J. Am. Soc. Mass Spectrom.* **2009**, *20*, 875.
- [19] Wu H. P., Su C. L., Chang H. C., Tseng W. L. Sample-first preparation: a method for surface-assisted laser desorption/ionization time-of-flight mass spectrometry analysis of cyclic oligosaccharides. *Anal. Chem.* **2007**, *79*, 6215.
- [20] Takayanagi T. Analysis of chemical equilibria in aqueous solution related with separation development using capillary zone electrophoresis. *Chromatography*, **2005**, *26*, 11.
- [21] Malehiat S., Brodbelt J. Cavity-size-dependent dissociation of crown ether/ammonium ion complexes in the gas phase. *J. Am. Chem. Soc.* **1993**, *115*, 2837. 1375–1380.